PLASMONIC MICROPILLARS FOR MASSIVELY PARALLEL PRECISION CELL FORCE MEASUREMENT

Fan Xiao[1], Ximiao Wen[1], and Pei-Yu Chiou[1,2]*

[1]Department of Mechanical and Aerospace Engineering, University of California, Los Angeles, Los Angeles, CA 90095, USA

[2]Department of Bioengineering, University of California, Los Angeles, Los Angeles, CA 90095, USA

ABSTRACT

A novel gold nanoparticle embedded plasmonic micropillar (PEM) platform for large area, massively parallel, and high-precision cell force measurement is demonstrated. Gold nanoparticles implanted into PDMS micropillars by laser pulses serve as strong and point-source-like scattering centers in dark-field imaging. These mechanically anchored gold nanoparticles are physically robust and chemically stable. Precision tracking of micropillars can be realized under a low numerical aperture (NA) objective lens for simultaneous and parallel measurement of cell traction forces across a large area. A spatial resolution of 30nm for pillar deflection measurement has been accomplished with a 20× objective lens.

INTRODUCTION

Mechanical interactions between cells and extracellular matrix environment (ECM) are critical for tissue functions. Several tools have been developed for measuring the interaction forces between cells and extracellular matrix. Atomic force microscopy can provide high sensitivity and high spatial resolution measurement, but with limited throughputs [1]. Elastomer substrates with embedded markers are easy to fabricate but requiring complex computation algorithms to extract cell traction forces [2]. Elastomer based micropillars platform is a broadly applied method since cell traction forces can be extracted from pillar deflection through a simple classical elasticity theory [3]. In prior micropillar works, the tips of elastomer micropillars are usually labeled with fluorescent markers to facilitate the identification of pillar locations [4, 5]. This approach, however, suffers few drawbacks [6-8]. The fluorescence proteins coated on pillars may degrade over time. The coating uniformity and thus the fluorescence intensity profiles on different pillars is also a concern. Both issues affect the accuracy of extracting force information from pillar locations, and a high NA and high magnification (60×~100×) objective lens is required for precision pillar tracking [9].

Here, we present a heterogeneously integrated, gold nanoparticle embedded plasmonic micropillar (PEM) platform to solve these issues on a pillar platform (Figure 1). PEM offers several unique advantages over prior works. Gold nanoparticles are extraordinary light scatters in the visible and NIR spectrum range due to their plasmonic effects[10-15]. This allows parallel monitor of a large number of cells and micropillars across a large area under a low NA objective lens. These gold nanoparticles are chemically stable and mechanically robust since they are locked inside micropillars. Fluorescence tracing marker degradation issues encountered in prior approaches are eliminated. Furthermore, the submicron sized gold nanoparticles are point-source-like light sources. The centers of these gold nanoparticles as well as the micropillar positions can be precisely determined with the commonly used Gaussian fitting method.

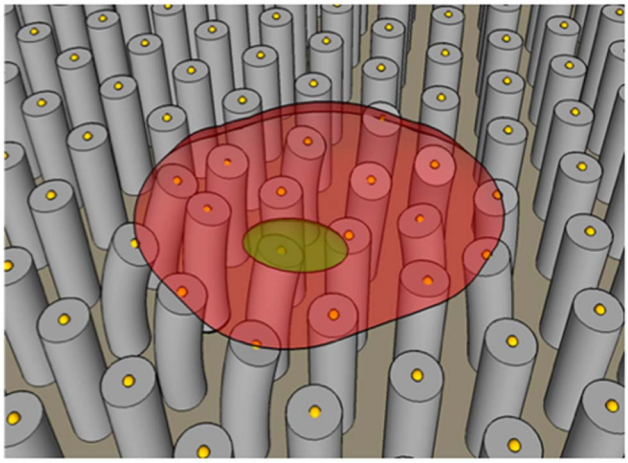

Figure 1: Schematics of a PEM platform for cell force measurement. The gold nanoparticles embedded in the PDMS elastomer pillars serve as point light sources to enable high spatial resolution pillar position tracking under a low magnification objective lens with a large field of view.

METHODS AND RESULTS

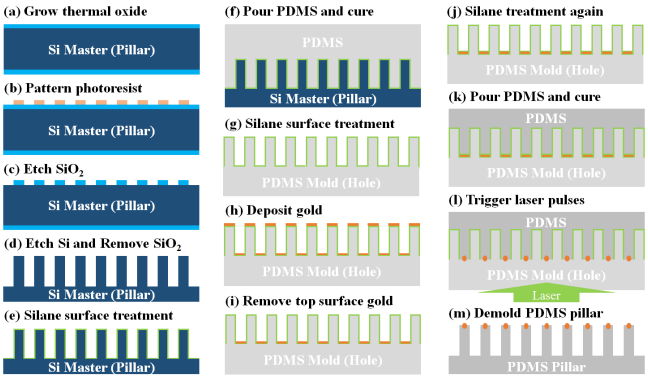

Figure 2: Fabrication process flow of plasmonic micropillar array.

The fabrication process flow of plasmonic micropillars is shown in Figure 2. It started from a silicon wafer with a

500nm thick thermal oxide (step a). The oxide layer was patterned to serve as the hard etch mask for the following deep reactive ion etching (DRIE, modified Bosch process) to create the silicon master mold (step b~d). The diameter (2 μm) and the height (10 μm) of the silicon pillars will determine the size of the later molded PDMS pillars. The thermal oxide layer was then etched away by hydrofluoric acid (HF) and placed in a vacuum chamber for silane coating. The chamber was degased for 1 hour and then left in vacuum overnight (step e). This surface treated silicon pillar array serves as a master mold for a following two-step replication process to fabricate the PDMS pillars.

Uncured PDMS precursor (degased Sylgard 184 elastomer and curing agent mixture at a w/w ratio 10:1) was poured on the silicon mold and cured at 80°C for 24 hours. This negative PDMS mold forms a microhole array that can be easily peeled off from the silicon mold. The PDMS mold was also silane treated overnight (step g). A composite layer of 20nm SiO_2/1nm Ti/40nm Au is deposited on the PDMS mold with an ebeam evaporator (CHA Mark 40, CHA Industries, Inc.) at a deposition rate of 1/0.2/1 Å/s (step h). Gold on top surface of PDMS mold was peeled off by a kapton tape (step i). Another silane surface treatment was carried out to facilitate the final demolding of PDMS pillars from the negative PDMS mold (step j). After treatment, degased uncured PDMS was poured on the PDMS mold and vacuumed to fill up the microholes. An oxygen plasma treated thin glass slide was covered on top of the uncured PDMS as a rigid substrate. After the device was cured in an oven at 80°C for 24 hours (step k), it was ready for the laser treatment.

Nanosecond laser induced gold melting, reshaping and transferring is critical in the fabrication process. The laser used in our experiment was a Q-switched, frequency doubled Nd:YAG pulse laser (Minilite I, Continuum) with a pulse width of 6ns and a wavelength of 532nm. Illuminated by a laser pulse with energy fluence at 400 mJ/cm^2, gold microdisks sandwiched between the PDMS pillars and mold were melted and evolved into nanoparticles due to surface tension. This process also detached them from the bottom PDMS holes and embedded them into the pillar tips (step l). This can be achieved by a single laser pulse. Finally, the gold nanoparticle embedded PDMS micropillar array was peeled off from the mold to finish the fabrication process (step m).

The optical and SEM images of the fabricated micropillars are shown in Figure 3(a) and 3(b). They confirm that there is only one gold nanoparticle embedded on each micropillar. The focused ion beam (FIB, Nova 600) image shown in Figure 3(c) shows that these embedded gold nanoparticles have an oblate spheroid shape with a long axis of 473nm and short axis of 268nm.

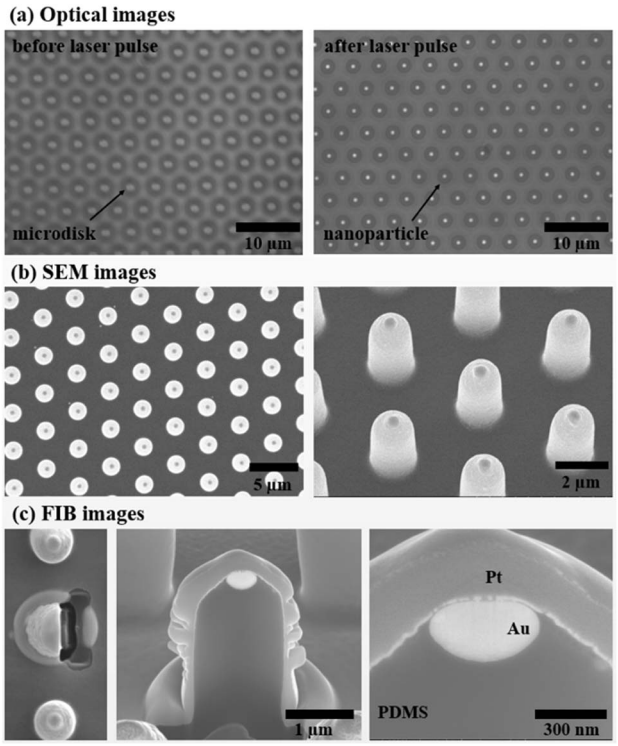

Figure 3: Micropillar structures on a PEM platform. (a) Microscopic optical images show the shape of gold nanoparticles before and after laser pulsing. (b) Scanning electron microscopic (SEM) images confirm that gold nanoparticles were transferred onto the pillar tips after laser pulsing. (c) Focus ion beam (FIB) images show that a transferred gold nanoparticle is physically anchored in the pillar and has an ablate spheroid shape with a long axis of 473nm and short axis of 268nm. Platinum (Pt) coating shown in the images is for FIB imaging and not a part of the original pillar structure.

Figure 4(a) shows a dark-field image of a PEM platform taken by a 20×, NA 0.5 objective lens. The illumination light source is a halogen lamp. The optical resolution of this system can be calculated by the Rayleigh criterion, 0.61λ/NA, where λ is the wavelength of light used for imaging and NA is the numerical aperture of the objective lens. Since the gold nanoparticle embedded in the pillar tip is smaller than the optical diffraction limit of this objective lens in the visible light range. The captured dark-field image of a gold nanoparticle by this 20× objective lens can be treated as a point source.

The intensity profile of a point source in an optical system can be described by the Airy point spread function (PSF). However, its calculation is tedious and in many practical applications, the PSF is approximated by a two-dimensional Gaussian function. A standard least-square fitting method is used in the current work for tracking gold nanoparticle locations at a sub-pixel resolution. The fitting precision depends on the relative scattering light intensity between a gold nanoparticle and its surrounding background

noises. Compared with gold nanoparticles, the PDMS micropillars and cells have small refractive index difference from the surrounding liquid media. The scattering light signals from them are weak and can be neglected. Figure 4(b) shows an example of sub-pixel resolution tracking of a gold nanoparticle by utilizing a two-dimension Gaussian function to fit the digitalized intensity profile.

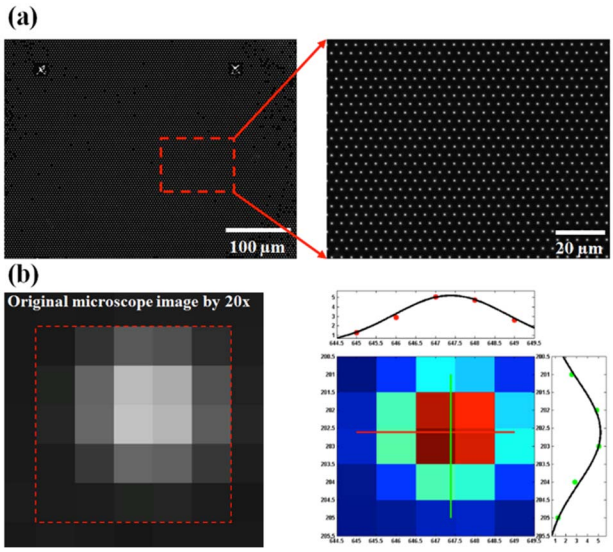

Figure 4: Sub-pixel resolution position measurement (a) Dark-field images of a PEM platform taken by a 20× objective lens (NA 0.5). (b) A zoom-in image of a single gold nanoparticle. Each square pixel represents a dimension of 322.5nm × 322.5nm in the dark-field image. The center location of this gold nanoparticle can be accurately measured at a sub-pixel resolution by using the 2D Gaussian fitting method.

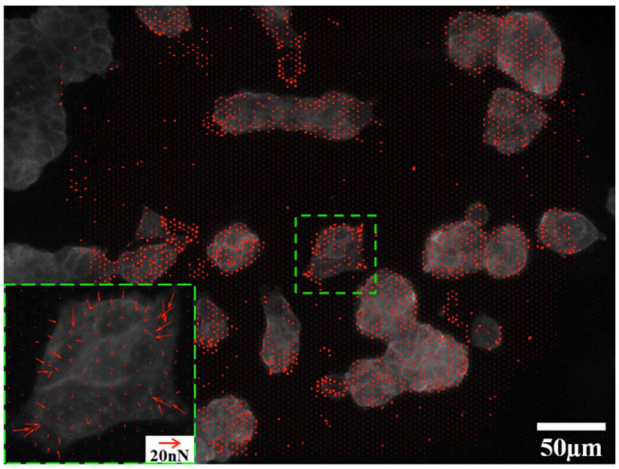

Figure 5: Representative force vector plots on cells (Madin-Darby canine kidney (MDCK, Sigma-Aldrich) spread on a PEM platform. A stacked image (dark field + fluorescence + force map) shows the magnitude and the direction of forces (length and direction red arrow) on micropillars.

The cell traction force on a pillar can be calculated by multiplying the pillar deflection by its spring constant. For a long cylindrical micropillar demonstrated in the current work, the force can be calculated by the following formula

$$F = \frac{4}{3}\pi E \frac{r^4}{L^3} \Delta x$$

where F is the horizontal traction force, E is the Young's modulus, r and L are the radius and height of the pillar, and Δx is the pillar deflection measured at the tip. For example, if a PDMS micropillar with a dimension of 2 μm in diameter, 10 μm in height, and E of 1 MPa, the 30 nm spatial resolution corresponds to a force measurement resolution of 0.36 nN.

To measure the cell force distribution on pillars, a reference image before cell loading is aligned with an image after cell loading. The deflections of pillars were obtained by subtracting the locations of the corresponding pillars in these two images. Figure 5 presents an example of force map of cells cultured on a PEM platform. The image FOV captured by the CCD camera is 448 μm × 333 μm; and the micropillar is 1.7 μm in diameter, 5.8 μm in height, and the pitch between pillars is 4 μm.

CONCLUSION

The novel plasmonic elastomer micropillar (PEM) platform demonstrated here solves some technical issues encountered in prior pillar approaches for massively parallel and precision cell force measurement in a large area. Gold nanoparticles embedded in pillars are chemically stable and mechanically robust, and extraordinary light scatters for dark field imaging. The submicron-sized gold nanoparticles are point-source-like light sources. The centers of these gold nanoparticles as well as the micropillar positions can be precisely determined with the commonly used Gaussian fitting method even under a low magnification objective lens. A spatial resolution of 30nm for pillar deflection measurement has been accomplished with a 20×, NA 0.5 objective lens.

ACKNOWLEDGEMENTS

This work is supported in parts by NIH R01 NX087494, NSF CBET-1404080, and NSF DBI 1256178.

REFERENCES

[1] S. E. Cross, Y. S. Jin, J. Rao, and J. K. Gimzewski, "Nanomechanical analysis of cells from cancer patients," *Nature Nanotechnology,* vol. 2, pp. 780-783, 2007.

[2] N. Q. Balaban, U. S. Schwarz, D. Riveline, P. Goichberg, G. Tzur, I. Sabanay, *et al.*, "Force and focal adhesion assembly: a close relationship studied using elastic micropatterned substrates," *Nature Cell Biology,* vol. 3, pp. 466-472, 2001.

[3] J. L. Tan, J. Tien, D. M. Pirone, D. S. Gray, K. Bhadriraju, and C. S. Chen, "Cells lying on a bed of microneedles: An approach to isolate mechanical force," *Proceedings of the National Academy of*

Sciences of the United States of America, vol. 100, pp. 1484-1489, 2003.
[4] J. P. Fu, Y. K. Wang, M. T. Yang, R. A. Desai, X. A. Yu, Z. J. Liu*, et al.*, "Mechanical regulation of cell function with geometrically modulated elastomeric substrates," *Nature Methods,* vol. 7, pp. 733-736, 2010.
[5] S. R. K. Vedula, M. C. Leong, T. L. Lai, P. Hersen, A. J. Kabla, C. T. Lim*, et al.*, "Emerging modes of collective cell migration induced by geometrical constraints," *Proceedings of the National Academy of Sciences of the United States of America,* vol. 109, pp. 12974-12979, 2012.
[6] K. A. Addae-Mensah, N. J. Kassebaum, M. J. Bowers, R. S. Reiserer, S. J. Rosenthal, P. E. Moore*, et al.*, "A flexible, quantum dot-labeled cantilever post array for studying cellular microforces," *Sensors and Actuators a-Physical,* vol. 136, pp. 385-397, 2007.
[7] B. G. Ricart, M. T. Yang, C. A. Hunter, C. S. Chen, and D. A. Hammer, "Measuring Traction Forces of Motile Dendritic Cells on Micropost Arrays," *Biophysical Journal,* vol. 101, pp. 2620-2628, 2011.
[8] C. M. Nelson, S. Raghavan, J. L. Tan, and C. S. Chen, "Degradation of micropatterned surfaces by cell-dependent and -independent processes," *Langmuir,* vol. 19, pp. 1493-1499, 2003.
[9] M. K. Cheezum, W. F. Walker, and W. H. Guilford, "Quantitative comparison of algorithms for tracking single fluorescent particles," *Biophysical Journal,* vol. 81, pp. 2378-2388, 2001.
[10] S. Link and M. A. El-Sayed, "Spectral properties and relaxation dynamics of surface plasmon electronic oscillations in gold and silver nanodots and nanorods," *Journal of Physical Chemistry B,* vol. 103, pp. 8410-8426, 1999.
[11] S. T. Wang, K. J. Chen, T. H. Wu, H. Wang, W. Y. Lin, M. Ohashi*, et al.*, "Photothermal Effects of Supramolecularly Assembled Gold Nanoparticles for the Targeted Treatment of Cancer Cells," *Angewandte Chemie-International Edition,* vol. 49, pp. 3777-3781, 2010.
[12] J. L. West and N. J. Halas, "Applications of nanotechnology to biotechnology - Commentary," *Current Opinion in Biotechnology,* vol. 11, pp. 215-217, 2000.
[13] V. P. Zharov, R. R. Letfullin, and E. N. Galitovskaya, "Microbubbles-overlapping mode for laser killing of cancer cells with absorbing nanoparticle clusters," *Journal of Physics D-Applied Physics,* vol. 38, pp. 2571-2581, 2005.
[14] S. E. Lee and L. P. Lee, "Biomolecular plasmonics for quantitative biology and nanomedicine," *Current Opinion in Biotechnology,* vol. 21, pp. 489-497, 2010.
[15] T. H. Wu, S. Kalim, C. Callahan, M. A. Teitell, and P. Y. Chiou, "Image patterned molecular delivery into live cells using gold particle coated substrates," *Optics Express,* vol. 18, pp. 938-946, 2010.

CONTACT

*P. Y. Chiou, tel:+1-310-825-8620; pychiou@seas.ucla.edu